

# PREDICTING TEMPERATURE AND LOADING RATE EFFECTS ON CLEAVAGE TOUGHNESS OF A STRUCTURAL STEEL USING A NEW LOCAL APPROACH MODEL

S. R. Bordet  
TWI, Granta Park, Great Abington, Cambridge, CB1 6AL, UK

## ABSTRACT

The author recently proposed a new Local Approach model for cleavage fracture in steel, based on a new statistical local criterion, which expresses the necessity of simultaneously fulfilling the conditions for both microcrack nucleation and propagation for cleavage to occur. In this paper, it is shown that the new model has the potential of correctly quantifying the effects of size, constraint, temperature and loading rate on the risk of cleavage fracture of a modern offshore structural steel (BS 7191: Grade 450 EMZ).

## 1 INTRODUCTION

In a series of recent publications, the author [1-4] argued that most difficulties and inconsistencies encountered when applying existing micromechanical models of cleavage in steel resulted from the choice of the local fracture criterion, typically defined as the attainment of a critical value of stress in some part of the plastic zone (see Beremin [5]) usually referred to as the fracture process zone (FPZ). This dual criterion rightly reflects the well-accepted experimental evidence that plastic flow is a necessary precursor to cleavage, in that it conditions, or at least promotes, microcrack nucleation, and that a minimum level of stress needs to be applied locally to propagate these cracks. However, such a definition leaves out many fundamental characteristics of cleavage, which are also well-established experimentally, notably that microcracks are continuously created with plastic deformation, that the microcrack nucleation rate increases with the material's yield strength (i.e. with decreasing temperature and increasing strain rate) and that only freshly nucleated microcracks are capable of propagation [1-4]. This last characteristic suggests the necessity of a dynamic continuity between the nucleation and propagation stages for cleavage to occur. This is easily reconciled with the idea that an arrested or slow moving crack is rapidly blunted by the ductile ferritic matrix. Only fast propagating cracks, whose high strain rates at their tip prevent dislocation emission, are compatible with sustained unstable propagation, hence the very existence of a characteristic 'critical stress' (more correctly 'statistical distribution of critical stresses') for cleavage fracture, largely independent of temperature, strain rate and constraint [1].

## 2 PRESENTATION OF THE NEW LOCAL APPROACH MODEL

Considering that a critical stress criterion suitably characterises the propagation stage of cleavage, the new local criterion attempts to better account for the nucleation stage, with which the above missing characteristics are primarily associated. Based on experimental evidence and by way of simplification, the nucleation stage is assumed to be a function of plastic strain only, which is independent of the level of stress and triaxiality. Within an infinitesimal volume  $dV$  of the FPZ, the probability of microcrack nucleation over a small plastic strain increment  $d\varepsilon_p$  is defined as [1,3]:

$$\delta P_{nuc}(\varepsilon_p) \propto \frac{\sigma_{ys}}{\sigma_{ys,0}} \exp\left(-\frac{\sigma_{ys}}{\sigma_{ys,0}} \cdot \frac{\varepsilon_p}{\varepsilon_{p,0}}\right) d\varepsilon_p dV$$

where  $\sigma_{ys}$  is the yield strength at the temperature and strain rate under consideration,  $\varepsilon_p$  is the equivalent plastic strain,  $\sigma_{ys,0}$  is a reference yield strength and  $\varepsilon_{p,0}$  is a scaling parameter. The exponential term corresponds to the reduction in available nucleation sites (e.g. carbides) as each site can be activated only once through plastic straining (each carbide may contain several potential nucleation sites). Assuming that the nucleated microcracks can be treated as Griffith flaws, size-distributed as an inverse power law, the probability of propagation is expressed as:

$$\begin{cases} P_{propag}(\sigma_1) = 0 & \sigma_1 < \sigma_{th} \\ P_{propag}(\sigma_1) \propto \sigma_1^m - \sigma_{th}^m & \sigma_1 \geq \sigma_{th} \end{cases}$$

where  $\sigma_1$  is the maximum principal stress and  $\sigma_{th}$  is the threshold local stress for cleavage propagation. Assuming that both stages are statistically independent, the probability of cleavage fracture of an elementary volume  $dV$  is:

$$P_{cleav} = \int_0^{\varepsilon_{p,u}} P_{propag} \cdot \delta P_{nucl} = \int_0^{\varepsilon_{p,u}} \frac{\sigma_{ys}}{\sigma_{ys,0}} \exp\left(-\frac{\sigma_{ys}}{\sigma_{ys,0}} \cdot \frac{\varepsilon_p}{\varepsilon_{p,0}}\right) \cdot \left(\left(\frac{\sigma_1}{\sigma_u^*}\right)^m - \left(\frac{\sigma_{th}}{\sigma_u^*}\right)^m\right) \frac{dV}{V_0} d\varepsilon_p \quad (1)$$

where  $\varepsilon_{p,u}$  is the equivalent plastic strain in  $dV$  at load time  $t$  and  $\sigma_u^*$  is a scaling parameter. Eqn (1) clearly states that conditions for microcrack nucleation and propagation need to be simultaneously met to have any chance of inducing cleavage. It also implies that microcrack nucleation under insufficient stress (i.e. when  $\sigma_1 < \sigma_{th}$ ) leads to a prestrain effect through a reduction in available nucleation sites (as expressed by the exponential term) which will then have to be counterbalanced by an increased average fracture stress. Invoking the weakest-link principle over the FPZ volume,  $V_p$ , for which  $\sigma_1 > \sigma_{th}$ , the global cleavage probability,  $P_f$ , is expressed as a Weibull distribution:

$$P_f = 1 - \exp\left(-\left(\frac{\sigma_w^*}{\sigma_u^*}\right)^m\right) \quad (2)$$

where  $m$  and  $\sigma_u^*$  are material parameters and  $\sigma_w^*$  is a modified Weibull stress given by:

$$\sigma_w^* = \left\{ \int_{V_p} \left( \int_0^{\varepsilon_{p,u}} \frac{\sigma_{ys}}{\sigma_{ys,0}} (\sigma_1^m - \sigma_{th}^m) \exp\left(-\frac{\sigma_{ys}}{\sigma_{ys,0}} \cdot \frac{\varepsilon_p}{\varepsilon_{p,0}}\right) d\varepsilon_p \right) \frac{dV}{V_0} \right\}^{1/m}$$

Thereafter, it is assumed that the ratio  $\sigma_{ys,0} \cdot \varepsilon_{p,0} / \sigma_{ys}$  is sufficiently large relative to the actual critical  $\varepsilon_p$ -values (i.e. the number of de-activated nucleation sites is sufficiently low compared with the number of nucleation sites still available) so that  $\sigma_w^*$  can be simplified as:

$$\sigma_w^* = \left\{ \int_{V_p} \left( \int_0^{\varepsilon_{p,u}} \frac{\sigma_{ys}}{\sigma_{ys,0}} (\sigma_1^m - \sigma_{th}^m) d\varepsilon_p \right) \frac{dV}{V_0} \right\}^{1/m} \quad (3)$$

### 3 PREDICTING TEMPERATURE EFFECTS ON CLEAVAGE TOUGHNESS

The new model was applied to predict the lower-shelf toughness transition curve of a modern structural steel plate (Grade 450 EMZ), obtained from the testing of deep-notched Single Edge Notch Bend (SENB) specimens, both under quasi-static and dynamic loading conditions. The steel was produced to BS 7191 [6] so as to obtain a fine-grained mixed microstructure of ferrite and bainite. All experimental data and finite element (FE) models are presented in detail in [4]. The model parameters were calibrated using notched tensile (NT) fracture specimens tested at  $-196^\circ\text{C}$ . The modified Weibull stress,  $\sigma_w^*$ , was calculated numerically from the FE results as follows:

$$\sigma_w^* = \left( \sum_{j=1}^{n_e} \sum_{i=1}^{n_{ip,j}} \left( \sum_{l=1}^{n_l} \frac{\sigma_{ys}(\bar{\dot{\epsilon}}_{i,j}(l))}{\sigma_{ys,0}} \text{Max}(\bar{\sigma}_{1,i,j}(l) - \sigma_{th}^m, 0) \Delta \varepsilon_{p,i,j}(l) \frac{V_{i,j}}{V_0} \right) \right)^{1/m}$$

where  $\bar{\dot{\epsilon}}_{i,j}(l) = (\dot{\epsilon}_{i,j}(l) + \dot{\epsilon}_{i,j}(l-1))/2$  is the averaged strain rate,  $\bar{\sigma}_{1,i,j}(l) = (\sigma_{1,i,j}(l) + \sigma_{1,i,j}(l-1))/2$  is the averaged maximum principal stress and  $\Delta \varepsilon_{p,i,j}(l) = \varepsilon_{p,i,j}(l) - \varepsilon_{p,i,j}(l-1)$  is the plastic strain increment at integration Gauss point (IP)  $i$  within element  $j$  between load step numbers  $l-1$  and  $l$  of the FE analysis (in the dynamic case,  $l$  represents the actual time).  $n_l$  is the current load step number,  $n_e$  is the number of elements in the volume delimiting the fracture process zone,  $n_{ip,j}$  is the number of IPs for element  $j$  and  $V_{i,j}$  is the IP volume in element  $j$ .  $\sigma_{ys,0}$  was given the value of the quasi-static yield strength at  $-196^\circ\text{C}$  and the reference volume  $V_0$  was conveniently fixed to one unit volume for all calculations. The maximum load increment allowed in the FE calculations was set in such a way as to leave  $\sigma_w^*$  relatively unchanged when reduced to a smaller increment size. Because  $\sigma_w^*$  is a function of  $m$ , the latter was calibrated using an iterative procedure similar to that proposed by Minami et al. [7]. Sets of  $\sigma_w^*$ -values at failure were calculated by linking each diametrical contraction recorded experimentally with that of the FE model. The maximum likelihood method was then employed to estimate  $m$  from the set of  $\sigma_w^*$ -values, until the  $m$ -estimate matched the value assumed in the calculation of  $\sigma_w^*$ . The value of the  $m$ -estimate is very sensitive to the choice of the threshold stress  $\sigma_{th}$ . The value for  $\sigma_{th}$  was fixed so that the  $\sigma_w^*$ -values in eqn (2) (representing 63.2% risk of fracture) were approximately the same in the NT and in the SENB geometry, tested at the same temperature of  $-196^\circ\text{C}$ . The following unbiased estimates were obtained:  $m_{e,unb} = 11.2$ ,  $\sigma_u^* = 2632$  MPa and  $\sigma_{th} = 1570$  MPa. The 95% confidence intervals for  $m_{e,unb}$  and  $\sigma_u^*$  were [6.9, 18.1] and [2502, 2768] respectively.

Figure 1a represents a comparison between toughness results obtained on  $50 \times 50$  mm<sup>2</sup> SENB specimens and the predictions calculated from eqn (2) using the material parameters determined at  $-196^\circ\text{C}$ : the only varying parameter is the yield strength, whose evolution with temperature was obtained experimentally [4]. One observes that the toughness predictions are in good agreement with measured values, given that the model is only supposed to capture the main lower shelf (pure cleavage) initiation mechanism (solid symbols). The 95% risk curve correctly predicts the change of fracture mode occurring at  $-130^\circ\text{C}$  between the pure cleavage initiation mechanism and the mixed ductile/cleavage initiation mechanism (open symbols), which is not predictable by the current model. At  $-130^\circ\text{C}$ , the number of measured  $\delta_c$ -values is sufficient to allow for acceptable statistical treatment. Figure 1b shows a comparison between the predicted evolution of  $P_f$  with CTOD (solid line) and median rank probabilities,  $P_i$ , for the measured  $\delta_c$ -values at  $-130^\circ\text{C}$  (only toughness values corresponding to the pure cleavage initiation mechanism were considered).  $P_i$  was calculated using the best (approximate) estimate of the median rank probability  $P_i = (i - 0.3)/(N + 0.4)$ , where  $i$  denotes the rank number and  $N$  defines the total number of

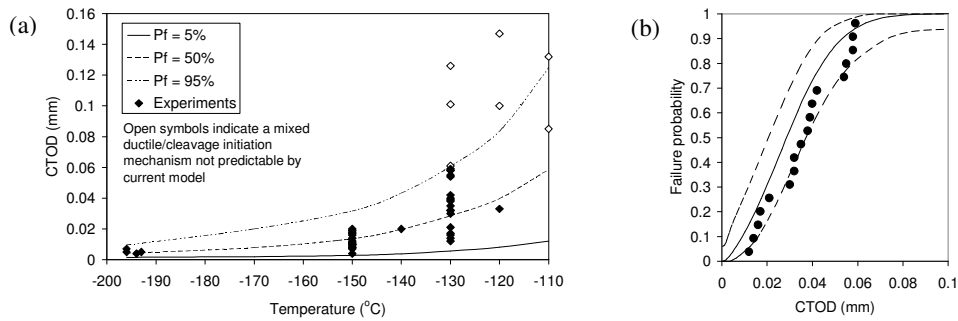


Figure 1: (a) Quasi-static lower shelf toughness predictions. (b) Comparison between predicted failure probabilities (solid line) and median rank probabilities for the pure cleavage  $\delta_c$ -results (filled symbols in (a)) at  $-130^\circ\text{C}$ . The dashed lines represent the 90% confidence limits for the rank probabilities.

fracture tests. The dashed lines represent the 90% confidence limits for the estimates of the experimental rank probabilities. These confidence limits were computed assuming that  $P_f$ , given by eqn (2), provides the expected median rank probability for an experimental data set containing the number of measured values  $N$ . The numerical procedure to compute the 90% confidence limits follows Wallin [8]. The calibrated model fits the experimental data set relatively well, though being slightly over-conservative: this is expected since the persistence of a linear relationship between the microcrack nucleation rate and the yield strength is increasingly over-optimistic as the temperature is raised and the ductile-brittle transition (DBT) region is approached [3-4].

#### 4 PREDICTING LOADING RATE EFFECTS ON CLEAVAGE TOUGHNESS

Figure 2a shows a comparison between toughness results of  $50 \times 50 \text{ mm}^2$  SENB specimens at load line velocity (LLV) of 10 mm/s and the predictions based on the same set of Weibull parameters determined from the quasi-static NT tests at  $-196^\circ\text{C}$ . As for the quasi-static case, the only varying parameter is the yield strength, whose evolution with temperature and strain rate was inferred from experiments [4]. Figure 2c presents the same comparisons for LLV = 120 mm/s. For both strain rates the predictions are in good general agreement. However, it is noticed that the results are increasingly underpredicted as the temperature is raised, although the targeted toughness values (solid symbols in Figures 2a and 2c) are within the range where the ‘pure cleavage’ type is expected to be the dominant initiation mechanism (cf. Figure 1a). Comparison of the predictions at  $-100^\circ\text{C}$  between Figures 2a and 2c shows that while this underprediction is pronounced for LLV = 10 mm/s, this is not the case for LLV = 120 mm/s. This is apparent in Figures 2b and 2d where  $P_f$  is compared with median rank probabilities for the dynamic  $\delta_c$ -results, which belong to the ‘pure cleavage’ category (solid symbols in Figures 2a and 2c). The model predicts the shape of the experimental toughness distribution well for both LLVs. However, whereas the model suitably predicts the position of the experimental toughness distribution with respect to CTOD for LLV = 120 mm/s, the predicted  $P_f$  curve is noticeably shifted to the left relative to the median rank probabilities for LLV = 10 mm/s, which is indicative of over-conservatism.

These discrepancies reflect the effects of temperature on work of fracture, stress relaxation, carbide debonding etc. [1,3], which become stronger as temperature is increased and which are not presently modelled. The fact that the model underpredicts dynamic CTOD ranges, which were suitably predicted in the quasi-static loading case, reveals that a higher strain rate cannot fully compensate for an increase in temperature. For example, due to thermally activated diffusional

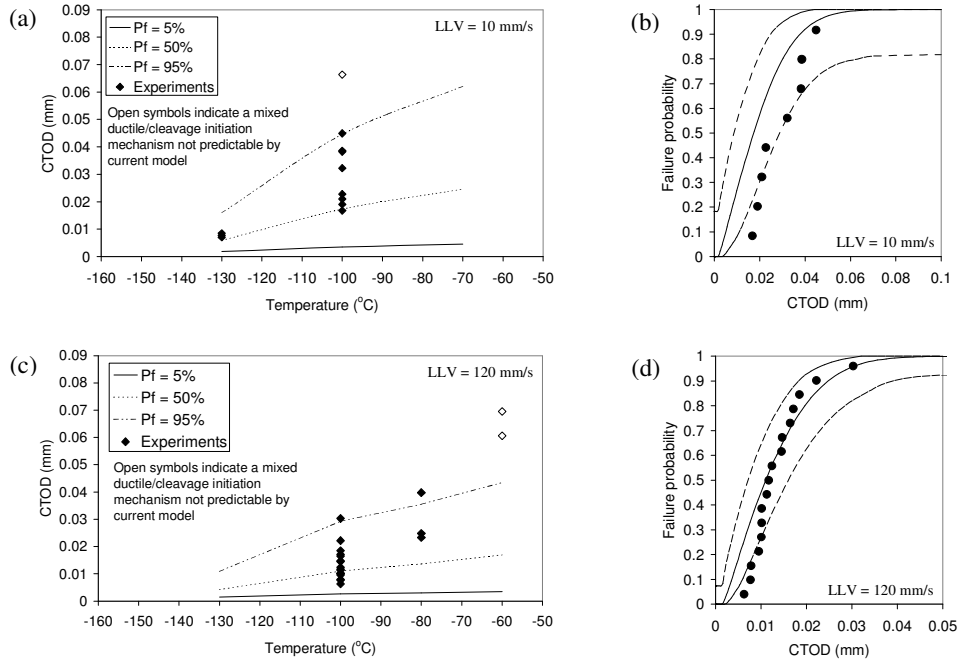


Figure 2: Dynamic lower shelf toughness predictions at (a) LLV = 10 mm/s and (c) LLV = 120 mm/s. Comparison between predicted failure probabilities (solid line) and median rank probabilities for the pure cleavage  $\delta_c$ -results (filled symbols in (a) and (c)) at  $-100^\circ\text{C}$  for (b) LLV = 10 mm/s and (d) LLV = 120 mm/s. The dashed lines represent the 90% confidence limits for the rank probabilities.

processes, a temperature shift  $\Delta T$ , causing the same change in yield strength as an imposed strain rate shift  $\Delta \dot{\epsilon}_p$ , will have a stronger effect on carbide stress relaxation than  $\Delta \dot{\epsilon}_p$ . Also, once a carbide crack or a ferrite microcrack is running, the strain rates generated at their tips are far superior to the strain rates imposed by the dynamic loading conditions, so that the temperature is likely to have stronger effects than  $\Delta \dot{\epsilon}_p$  for equivalent changes in yield strength. The work of fracture behind the moving cleavage crack, involving the elongation and rupture of ductile ligaments, will also vary more as a function of  $\Delta T$  than  $\Delta \dot{\epsilon}_p$ . The temperature shift observed between two toughness curves of the same steel at different strain rates is therefore smaller than what would be obtained if all temperature dependent parameters, with the exception of the yield strength, were kept constant. The model, which only considers the effect of temperature on the yield strength, will therefore predict a transition temperature higher than the actual one. As a result, the model will predict a lower shelf toughness region extending to temperatures for which the actual toughness already belongs to the fast increasing DBT region, which explains why the model increasingly underpredicts cleavage toughness as the temperature is raised in Figures 2a and 2c. This also explains why the model underpredicts experimental toughness data at  $-100^\circ\text{C}$  for LLV = 10 mm/s (Figure 2a), but not for LLV = 120 mm/s (Figure 2c), if one considers that the model overestimation of the probability of cleavage fracture at small probabilities in Figure 2d is

principally due to assuming  $\delta_{min} = 0$ . This arises from the fact that the higher the loading rate, the higher the ductile-brittle transition temperature. For LLV = 120 mm/s, the experimental cleavage toughness values at  $-100^{\circ}\text{C}$  still belong to the lower shelf, whereas those for LLV = 10 mm/s belong to the lower part of the DBT region, hence a greater gap with the model predictions in the second case. This gap can be considered to be accentuated even further by the fact that the FE analysis does not take into account deformation heat, which is all the less readily dissipated as the loading rate is higher (see e.g. Chiou [9]). At a given loading rate, the higher the test temperature, the higher the toughness and thus the plastic strains at the crack tip. Although the yield strength decreases with test temperature, the crack tip plastic strains increase at a comparatively much faster rate (the mean quasi-static  $\delta_c$ -value doubles between  $-150$  and  $-130^{\circ}\text{C}$ ), which results in a temperature elevation within the FPZ and a thermal softening of the local yield strength increasingly underestimated by the FE model as test temperature rises. This is even more the case at the loading rate of 10 mm/s, which is unlikely to thermally compensate for the smaller strains developing in the FPZ at the albeit faster rate of 120 mm/s [9].

## 5 CONCLUSION

A new Local Approach model was applied to predict the lower shelf toughness transition curve of a modern offshore structural steel plate (BS 7191: Grade 450 EMZ), under both quasi-static and dynamic conditions. The model parameters were calibrated from quasi-static notched tensile (NT) fracture specimens, tested at  $-196^{\circ}\text{C}$ . Good toughness predictions were obtained in the quasi-static case, validating the ability of the model to predict effects of size, constraint and temperature on cleavage fracture. The new model also showed potential for correctly predicting the effect of dynamic loading on cleavage toughness.

## REFERENCES

- [1] Bordet SR. Ph.D. thesis, University of Cambridge, 2002.
- [2] Bordet SR, Karstensen AD, Wiesner CS, Knowles DM. The Local Approach in structural integrity assessments: transforming its potential into an engineering tool. In: Flewitt PEJ et al. (Eds), *Engineering structural integrity assessment: needs and provision*, EMAS, pp. 253-60, 2002.
- [3] Bordet SR, Karstensen AD, Knowles DM, Wiesner CS. A new statistical local criterion for cleavage fracture in structural steel, Part I – Model presentation. To appear in *Eng Frac Mech*.
- [4] Bordet SR, Karstensen AD, Knowles DM, Wiesner CS. A new statistical local criterion for cleavage fracture in structural steel, Part II – Application to an offshore structural steel. To appear in *Eng Frac Mech*.
- [5] Beremin FM. A local criterion for cleavage fracture of a nuclear pressure vessel steel. *Met Trans A*, 14A, 2277-87, 1983.
- [6] British Standard, BS 7191: 1989. Weldable structural steels for fixed offshore structures. BSI, 1989.
- [7] Minami F, Brückner-Foit A, Munz D, Trollidenier B. Estimation procedure for the Weibull parameters used in the Local Approach. *Int J Fracture*, 54(3), 197-210, 1992.
- [8] Wallin K. Optimized estimation of the Weibull distribution parameters. Research report 604, Technical Research Centre of Finland, Espoo, Finland, 1989.
- [9] Chiou ST, Lee WS. Plastic deformation and fracture response of 304 stainless steel subjected to dynamic shear loading. *Mater Sci Tech*, 19(9), 1266-72, 2003.